Title
Competing magnetic anisotropies in an AFM-FM-AFM trilayer

Author
Bali, R.

Publication Date
2010-01-15

Peer reviewed

Competing magnetic anisotropies in an AFM-FM-AFM trilayer

R. Bali[1,*], B.B. Nelson-Cheeseman[2], A. Scholl[3], E. Arenholz[3], Y.Suzuki[2] and M.G. Blamire[1]

[1]*Department of Materials Science, University of Cambridge, Pembroke Street, CB2 3QZ, United Kingdom*

[2]*Department of Materials Science and Engineering, University of California, Berkeley, California 94720, USA*

[3]*Advanced Light Source, Lawrence Berkeley National Laboratory, Berkeley, California 94720, USA*

Abstract

An antiferromagnet-ferromagnet-antiferromagnet trilayer was grown in magnetic field using CoMn, Permalloy (Py) and FeMn respectively. Magnetometry studies show that the direction of exchange coupling of CoMn with Py was perpendicular to that of Py with FeMn. These results are explained by a spin-flop in the CoMn layer, and show that the spin structure of an antiferromagnet may undergo severe modification due to a relatively small magnetic field applied during its growth. The perpendicular exchange coupling was exploited in the CoMn-Py-FeMn trilayer to manipulate the easy axis of the ferromagnet.

[*] Present address: Max Planck Institute of Microstructure Physics, Weinberg 2, D-06120, Halle, Germany. Email: rbali@mpi-halle.mpg.de

Introduction

In multilayered devices, magnetic anisotropy plays a crucial role in determining the magneto-resistance signal. Owing to the technological significance of these devices it is important to control magnetic anisotropies, particularly when anisotropies from various sources compete and determine the direction of magnetization. Magnetic anisotropy in thin films may be dominated by magnetocrystalline, shape or strain effects. When these ferromagnetic thin films are incorporated into heterostructures, additional competing anisotropy contributions such as the composition of non-magnetic spacer layers,[1] lattice distortions at the interface[2] and perpendicular uniaxial and exchange anisotropies,[3] may be relevant. Exchange anisotropy is based on exchange coupling of a ferromagnetic layer with an adjacent layer, often an antiferromagnet, and has been exploited in magnetic tunnel junctions and spin valves. Exchange coupling with antiferromagnets induces exchange bias[4] which is sensitive to the interfaces and can be controlled by cooling through the Néel temperature (T_N) in the presence of magnetic field. Reversible manipulation of the direction of the FM easy axis, and hence the overall magnetic anisotropy, is of interest to the further development of magnetic devices.

Here we describe a new model system composed of a trilayer of AFM-FM-AFM where we can reversibly manipulate the magnetic anisotropy. The two AFM layers were CoMn and FeMn that have large difference in their blocking temperatures, while the FM was a Permalloy (Py, $Ni_{81}Fe_{19}$) layer which has minimal magnetocrystalline anisotropy. The magnetic anisotropy in the Py will depend largely on the competing anisotropies induced by magnetic field applied during thin film growth, magnetic field cooling (MFC), and

AFM-FM exchange coupling. Bulk magnetometry measurements were performed to probe the overall magnetic anisotropy by identifying the easy axis (EA) of the FM. Surface sensitive, element specific of X-ray magnetic circular dichroism (XMCD) was employed to observe magnetic domains in the individual layers. The application of a magnetic field during growth was found to strongly influence the anisotropy of the CoMn, through spin-flop of the AFM spins. Bilayers of Py-CoMn and Py-FeMn indicated that the EA induced in the Py layer by the CoMn was perpendicular to the EA from the FeMn. In a trilayer of CoMn-Py-FeMn, the overall magnetic anisotropy is determined by the details of the magnetic history. The ability to manipulate the magnetic anisotropy in such a way makes the AFM-FM-AFM promising for technological applications.

Experimental

Polycrystalline films were magnetron sputtered onto Si substrates in 0.5 Pa Ar at room temperature. During growth, a saturating magnetic field of 400 Oe was applied by attaching permanent magnets on the sample holder. A buffer layer of 20 nm of Cu was deposited on the Si substrate before depositing the subsequent magnetic films. We grew two types of samples: FM-AFM bilayer and AFM-FM-AFM trilayer heterostructures. Bilayers of Si/$CoMn_{(20\ nm)}$/$Py_{(3.5\ nm)}$, Si/$Py_{(3.5\ nm)}$/$CoMn_{(20\ nm)}$ and Si/$Py_{(3.5\ nm)}$/$FeMn_{(5\ nm)}$ were grown. The growth sequence had a profound effect on the direction of the EA in the Py layer. The AFM-FM-AFM trilayers were composed of Si/$CoMn_{(20\ nm)}$/$Py_{(3.5\ nm)}$/$FeMn_{(5\ nm)}$ (Fig. 1).

The CoMn layer had a blocking temperature ($T_{b,\mathrm{CoMn}}$) of ~300 K, below its T_N of ~360 K (ref. 5). The FeMn has a blocking temperature and T_N of ~480 K (ref. 6) and 502 K respectively (ref. 7). For given interface conditions and grain size, T_b is the temperature above which exchange bias disappears, and is lower than its T_N. The large difference in T_b of CoMn and FeMn enabled us to study Py coupled with both FeMn and CoMn from 77 to 300 K and Py coupled to FeMn alone between 300 to 473 K. The thickness of the FeMn layer was fixed at 5 nm, slightly lower than its critical thickness for maximum exchange pinning.[6] The exchange energy of CoMn is expected to be lower than that of FeMn (ref. 1). Therefore 20nm of CoMn and 5nm of FeMn were incorporated into the trilayers so that exchange anisotropy contributions from the AFM layers would be comparable.

Magnetization measurements were performed in a vibrating sample magnetometer (VSM) with a cryostat attachment. Orientation of the samples with respect to growth magnetic field (H_g) and magnetic field during cooling (H_{fc}) was tracked by using 4x6 mm rectangular rather than square Si chips. MFC was usually carried out by applying H_{fc} of 10 kOe while cooling from 473 K to 77 K. Magnetization (M) versus applied field (H) curves were measured while warming back to 473 K at 10 K increments. For zero field cooling (ZFC), the sample was cooled to 77 K without external magnetic field. Magnetic domain imaging was performed using X-ray Photoemission Electron Microscopy (XPEEM).

Results and Discussions

First we examine the behaviour of the bilayers, in particular the position of the EA in as-grown samples. Let us define the axis of H_g to be at 0° in angular space within the plane of the film. The orientation of the EA was determined by plotting in-plane M-H loops between 0 and 180°, and identifying the orientation with the remanence closest to the saturation value. For the as-grown Py-FeMn bilayer, the EA was positioned parallel to H_g and Fig.2(a) shows the EA hysteresis loop for this sample at 0°. Similarly, the EA for a Py-CoMn sample was also observed at 0°.

However, for the as-grown CoMn-Py bilayer the EA was at 90° perpendicular to H_g. Six samples were studied and they consistently gave this result. Apart from the EA at 90° to H_g, this bilayer had the same qualitative H_{ex} vs. T behaviour as that of Py-FeMn bilayer which is a well studied system.[6-12] In Fig. 2(a) the sign of exchange bias (H_{ex}) of the as-grown bilayers depended on the direction of Py moments prior to ZFC.

In order to understand the effect of each of the AFM layers on the Py, we measured hysteresis loops at every 10 K while warming and extracted the exchange field at each temperature. Fig 2(b) shows the T variation of H_{ex} for the bilayers and trilayer. The H_{ex} were extracted from the hysteresis loops along the easy axes of the samples. At 300 K the H_{ex} of the CoMn-Py sample was near zero and this was taken as the $T_{b,\mathrm{CoMn}}$. Figure 2(b) also shows H_{ex} vs T for the as grown trilayer. The overall T_b of the trilayer was close to 350 K, and below 300 K its H_{ex} rose steeply and crossed over the Py-FeMn bilayer at 240 K.

In order to understand the behaviour of the perpendicular exchange couples in the trilayer we observed the response of its EA to ZFC and MFC. Figure 3(a) shows the hysteresis loops measured at 120 K for the as-grown trilayer after ZFC. These loops were indicative of frustrated moments where the remanence is small due to randomized moments at zero field and commence rotation at a magnetic field value determined by the local anisotropy. The moments were saturated in a field of 10 kOe and MFC on the samples was always carried out with H_{fc} fixed at -10 kOe. The frustrated arrangement was erased by MFC from 473 K to 77 K.

Figures 3(b) and (c) show that the pinched loops were replaced by easy and hard axes loops after MFC. In Fig. 3(b), MFC was carried out with H_{fc} parallel to 0°, making it the EA position. When the sample was warmed and then ZFC to 77 K the EA rotated to 90°, as seen in the M-H curve of Fig. 3(c) measured after ZFC. Since the EA rotated towards the 90° position under thermal activation, this must be its ground position while 0° was a metastable position. Note that the 90° ground position corresponds to the EA of the as-grown CoMn-Py bilayer, perpendicular to H_g. This ground state is the lowest energy position for coherent moments, and does not always match the local energy minima seen in the frustrated moments of the as-grown trilayer.

In order to track the thermally activated rotation of the metastable axis, the remanent magnetization (M_r) was measured at 0 and 90° while warming, and is shown in Fig. 4. As the sample was warmed, the EA remained fixed until 300 K where EA initiated its rotation from 0 towards its ground position at 90°.

In an attempt to assist this thermally activated rotation, a magnetic field (H_{app}) was applied at 300 K. After the above procedure of stabilizing the EA of the trilayer in its metastable position of 0°, the sample was warmed and at 300 K an H_{app} = 500 Oe was applied in the 90° direction for a few seconds and switched off. The effect of H_{app} on the rotating EA of the trilayer was observed after ZFC. The EA was observed to have shifted from 0 to 135°, as shown in Fig. 5(a). This EA of 135° also rotated towards 90° under thermal activation when warmed above 300 K (Fig. 4).

We attempted to return to the as-grown state (that is, the pinched hysteresis loop shown in Fig. 3(a)) by applying a sharply oscillating and decreasing field. If the pinched loop of the as-grown trilayer was due to randomly oriented local moments, then sharp field oscillations could break the long range coherence of the moments and return them to their frustrated state. MFC was performed from 473 K to 300 K with H_{fc} // 0°, aiding the metastable axis. The -10 kOe field was then oscillated down to zero with 10% decrease in field at every oscillation and 30 Oe/sec rate. The sample was then cooled to 77 K in zero external field, to ZFC through $T_{b,\mathrm{CoMn}}$. Fig 5(b) shows the pinched hysteresis loop measured after warming to 120 K.

Magnetic domains in the bilayers and trilayers were studied at beamline 7.3.1 of the Advanced Light Source at the Lawrence Berkeley National Laboratory Laboratory to probe the moment orientations within each layer. Figures 6(a) and (b) show XPEEM images of the $CoMn_{(20\ nm)}$-$Py_{(2\ nm)}$. The mean probe depth of 5 nm meant that the thickness of the top layer had to be reduced from 3.5 nm to 2 nm to allow penetration of

X-ray light across the interface. The circularly polarized light beam was incident along the 0° direction.

Tuning to the Fe $L_{2,3}$ edges allowed us to observe magnetic domains in the Py film. Magnetic domains were observed separated by Néel walls (Fig. 6(a)). The domain walls showed strong contrast parallel to 0° thereby showing that the direction of moments within the domains was at 90° to H_g. The domains were surrounded by a region of ripple contrast, suggesting appreciable variation in local moment direction of this as-grown bilayer. By tuning to the Co $L_{2,3}$ edges uncompensated spins of the CoMn AFM were observed in the bilayer (Fig. 6(b)). These uncompensated Co moments closely replicated the Py domain pattern seen in Fig. 6(a). Uncompensated Co moments could be due to interdiffusion commonly observed in metallic multilayers.[13]

Tuning to the Ni $L_{2,3}$ edge allowed the observation of domains in the Py layer of the CoMn $_{(20\ nm)}$-Py $_{(2\ nm)}$-FeMn $_{(3\ nm)}$ trilayer (Fig. 6(c)). The FeMn thickness was reduced to improve contrast from underlying layers. Since the domain walls were not clearly visible in this image it was difficult to interpret the direction of the moments. The domain size in this trilayer was much smaller than that of the bilayer, due to the additional exchange energy induced by FeMn.

The perpendicular EA observed in CoMn-Py bilayers can be explained by the modification of the CoMn spin structure due to H_g. This modification will be different for CoMn-Py and Py-CoMn since in the former the AFM spins will act under the influence of H_g alone, while in the latter the behaviour of the AFM spins will also be influenced by the underlying FM spins. The influence of H_g is expected to be more severe for AFMs with low magnetocrystalline anisotropy. In the limiting case for an AFM with zero anisotropy, H_g can cause a spin-flop in the AFM since the lowest energy position for an AFM spin pair would be perpendicular to H_g, so that neither spin opposes H_g.[14] Since its growth was carried out near its Néel temperature, the magnetocrystalline anisotropy of CoMn would have been minimal, allowing H_g to significantly modify its spin structure and potentially causing a spin-flop. While spin-flop has been observed in AFMs under fields of several Tesla, [15-16] the present observations suggest that spin-flop can be induced in an AFM during growth near its T_b by applying much smaller magnetic fields.

This explanation only addresses collinear AFMs with low anisotropy, which is not necessarily the case here. The spin-structure of FeMn is non-collinear[17] and the perpendicular EA was not observed with FeMn-Py bilayers, probably because the growth temperature was more than 100 K below its T_b maintaining high AFM anisotropy. The non-collinear spin structure of FeMn has been shown to weakly influence exchange coupling with Py in epitaxial films.[18] The spin structure of CoMn has not been studied in detail in literature; however, these results show that it is strongly influenced by H_g.

The CoMn layer will transmit the EA to Py overlayer via parallel exchange coupling. Spin-flop coupling[19-21] between CoMn and Py is expected to coexist with the parallel exchange coupling. [22] Spin-flop coupling does not contribute to H_{ex} (ref. 22) and in case of dominant spin-flop coupling, H_{ex} is the result of atomic scale interface defects.[23] Interface defects will strongly influence the magnitude of H_{ex} (ref. 24), but will not determine the EA direction since their influence is expected to be randomly oriented. Regardless of the type of exchange coupling, the sharp difference in the EA behaviour of

CoMn-Py and Py-CoMn clearly shows that the magnetic field modification of the CoMn controls the EA of the Py layer.

The EA of Py was aligned perpendicular to H_g despite the field magnitude of 400 Oe being sufficient to saturate the Py layer (Fig. 2(a)). This observation that the EA can be induced in a direction different from that of the saturating growth field shows that the AFM layer in proximity of the FM exerts a stronger influence than an external saturating field.

As observed in the Py-FeMn bilayer (Fig. 2(a)), FeMn tends to align the Py moments parallel to H_g (ref. 25), and will compete with CoMn that aligns the moments perpendicular to H_g. This competition may result in the frustration observed in the as-grown trilayer (Fig. 3). The frustrated state was erased when the competition was destroyed, by MFC through $T_{b,\mathrm{CoMn}}$ and reinduced by fast reversal at the $T_{b,\mathrm{CoMn}}$. It was the underlying CoMn that fixed the ground state perpendicular to H_g for coherent Py moments in the trilayer. The Py moments gradually rotated towards the ground state under thermal activation above $T_{b,\mathrm{CoMn}}$, and it was possible to increase the magnitude of this rotation at a given temperature by applying a magnetic field parallel to the ground state (Fig. 4).

Perpendicular exchange couples in the AFM-FM-AFM trilayer grown in field with H_g // 0° was exploited to manipulate four anisotropy states: (1) the frustrated anisotropy state of the as-grown trilayer, (2) the coherent state with stable easy axis via magnetic field cooling with H_{fc} // 90° (3) the coherent state but with a metastable easy axis keeping H_{fc} // 0° and (4) metastable intermediate easy axis by applying a toggle field, H_{app} // 90°

at $T_{b,\mathrm{CoMn}}$. The coherent states (2), (3) and (4) could be reversibly controlled via temperature and field, whereas the frustrated state (1) was locally irreversible, but approximately reinstated over an average of the FM layer.

Conclusions

Magnetic anisotropy competition was probed in a model system of CoMn-Py-FeMn where CoMn-Py exchange coupling was perpendicular to that of Py-FeMn. This was due to modification in the spin structure of CoMn when grown in magnetic field without the presence of other magnetic layers. The direction of the Py easy axis in the CoMn-Py-FeMn trilayer was controlled by magnetic and zero field cooling through the blocking temperature of CoMn, and application of magnetic field during the thermally activated rotation of the easy axis. Such manipulation of the easy axis via field cooling may impart an additional degree of control in magnetic devices.

Acknowledgments

The Advanced Light Source is supported by the Director, Office of Science, Office of Basic Energy Sciences, of the U.S. Department of Energy under Contract No. DE-AC02-05CH11231. R.B. would like to thank Dr. K.G. Sandeman and Dr. R.C. Chopdekar for productive discussions. Travel grants from Pembroke College Cambridge and Cambridge Philosophical Society are gratefully acknowledged.

References

[1] B. Skubic *et al.*, *Phys. Rev. Lett.* 96, 057205 (2006).

[2] H. Hafermann *et al.*, *Appl. Phys. Lett.* 94, 073102 (2009).

[3] Xiaosong Ji and Kannan M. Krishnan, *J. Appl. Phys.* 99, 08C105 (2006).

[4] J. Nogués and I. K. Schuller, *J. Magn. Magn. Mater.* 192, 203 (1999).

[5] M. Acet *et al.*, *J. Appl. Phys*. 70, 6556 (1991).

[6] Oletta Allegranza and Mao-Min Chen, *J. Appl. Phys.* 73, 6218 (1993)

[7] Takasu Hashimoto and Yoshikazu Ishikawa, *J. Phys. Soc. Jpn.* 23 pp. 213-223 (1967)

[8] C. Tsang and Kenneth Lee, *J. Appl. Phys.* 53, 2605 (1982).

[9] R.D. Hempstead, S. Krongelb, D.A. Thompson, *IEEE Trans. Magn.*14, 521 (1978).

[10] C. Schlenker *et al.*, *J. Magn. Magn. Mater.* 54-57, 801 (1986).

[11] J.K. Howard, T.C. Huang, *J. Appl. Phys.* 64, 6118 (1988).

[12] W. Stoecklein, S.S.P. Parkin, J.C. Scott, *Phys. Rev. B* 38, 6847 (1988).

[13] Xing-zhao Ding *et al.*, *J. Appl. Phys.* 85, 8322 (1999).

[14] Assuming zero uniaxial anisotropy, the energy equation of a spin pair s_1 and s_2 at angles ϕ_1 and ϕ_2 w.r.t H_g is:

$$E = -s_1 H_g \cos\phi_1 - s_2 H_g \cos\phi_2 - j\cos(\phi_1 - \phi_2)$$

where the exchange coupling coefficient j, is negative for AFM coupled spins. For spins of equal magnitude ($s_1 = s_2$), this energy is minimum when $\phi_1 = -\phi_2$ and $\phi_1 - \phi_2$ = 180°, giving ϕ_1 = 90° and ϕ_2 = -90° which is the spin-flopped state.

[15] Y. Shapira and S. Foner, *Phys. Rev. B* 1, 3083 (1970).

[16] J. Nogués, L. Morellon, C. Leighton, M. R. Ibarra, and Ivan K. Schuller, *Phys. Rev. B* 61, R6455 (2000).

[17] W. Kuch *et al.*, *Phys. Rev. Lett.* 92, 017201 (2004).

[18] R. Jungblut, *J. Appl. Phys*. 75 (10), 6659 (1994).

[19] N. C. Koon, Phys. Rev. Lett. 78, 4865 (1997).

[20] T. J. Moran *et al.*, *Appl. Phys. Lett.* 72, 617 (1998).

[21] Elke Arenholz *et al.*, *Phys. Rev. Lett.* 98, 197201 (2007).

[22] M. D. Stiles and R. D. McMichael, *Phys. Rev. B* 59, 3722 - 3733 (1999).

[23] T. C. Schulthess and W. H. Butler, *Phys. Rev. Lett.* 81, 4516 - 4519 (1998).

[24] W. Kuch *et al.*, *Nature Materials* 5, (2), pp 128-133 (2006).

[25] W. J. Antel, Jr., F. Perjeru, and G. R. Harp, *Phys. Rev. Lett.* 83, 1439 - 1442 (1999).

LIST OF FIGURES

FIG. 1 (color online): The trilayer with CoMn (20 nm), Py (3.5 nm) and FeMn (5 nm) grown in the presence of magnetic field H_g. Black arrows indicate the expected direction of CoMn spins, perpendicular to H_g and uncompensated Co spins close to Py interface.

FIG. 2 (color online): (a) Easy axis hysteresis loops for bi-layered samples, showing H_{ex}. The CoMn-Py layer had its EA perpendicular to the growth field, while in the case of $Py_{(3.5\ nm)}$-$FeMn_{(5\ nm)}$ the EA was parallel to growth field (b) Easy axis H_{ex} vs. T variation for bilayers and trilayer showing T_b = 300 K for the CoMn-Py bilayer.

FIG. 3 (color online): (a) Easy and hard axis loops for the as-grown $CoMn_{(20\ nm)}$-$Py_{(3.5\ nm)}$-$FeMn_{(5\ nm)}$ trilayer after ZFC to 120 K (b) effect of MFC from 473 K to 120 K in –10 kOe with H_{fc} // 0° (c) subsequent ZFC to rotate the EA to its ground position at 90°.

FIG. 4 (color online): Temperature variation of M_r after MFC with H_{fc} // 0°. M_r was measured at 0° and 90° while warming the sample. The 135° line was measured in a separate run, with the same MFC as previous. At 300 K, H_{app} was applied at 90° rotating the EA to 135°. The sample was cooled and M_r measured at 135° while warming.

FIG. 5 (color online): (a) Stable EA created at 135° by applying a field (H_{app}) at $T_{b,\mathrm{CoMn}}$ and ZFC to 120 K. (b) Effect of sharply oscillating and decreasing field and ZFC to 120 K.

FIG. 6: XPEEM images of (a) Magnetic contrast in the Py layer and (b) uncompensated Co spins in the CoMn of the CoMn-Py bilayer; (c) Magnetic domains in the Py of the CoMn-Py-FeMn trilayer.

FIG. 1

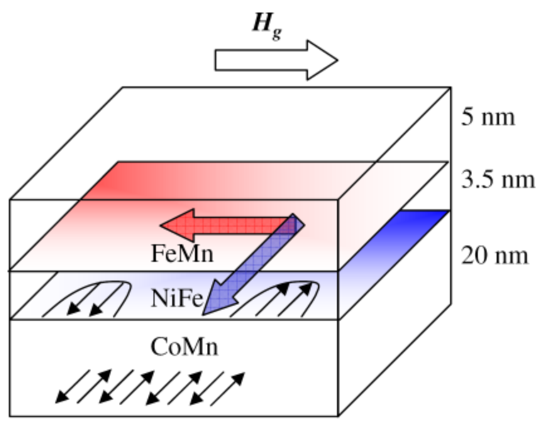

FIG. 2

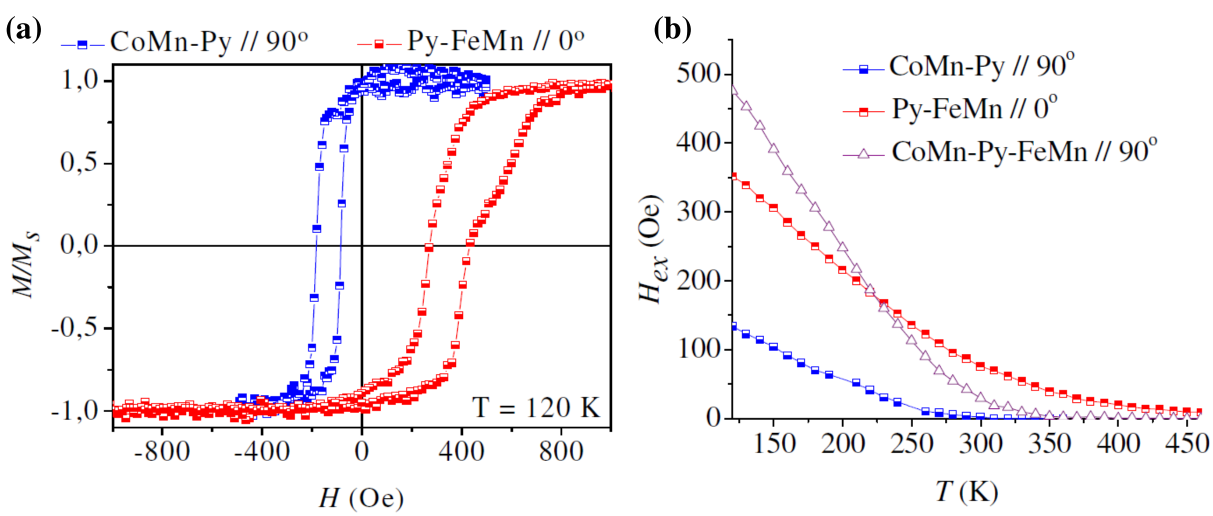

(a)
CoMn-Py // 90°
Py-FeMn // 0°
1,0
0,5
0,0
-0,5
-1,0
M/M_S
-800
-400
0
400
800
H (Oe)
T = 120 K
(b)
CoMn-Py // 90°
Py-FeMn // 0°
CoMn-Py-FeMn // 90°
500
400
300
200
100
0
H_ex (Oe)
150
200
250
300
350
400
450
T (K)

FIG. 3

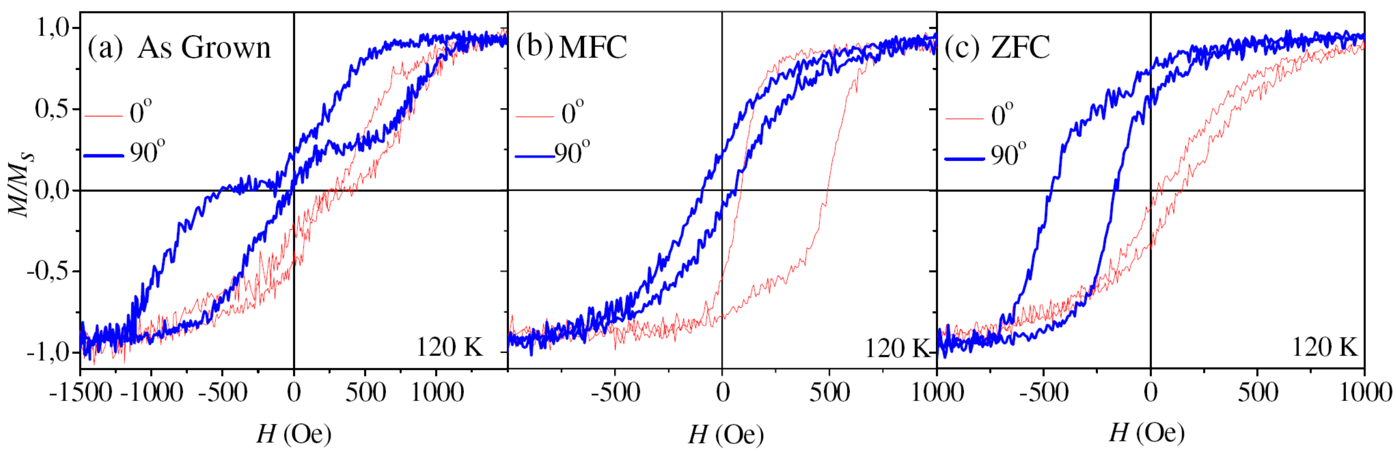

(a) As Grown
0°
90°
120 K
(b) MFC
0°
90°
120 K
(c) ZFC
0°
90°
120 K
M/M_S
1,0
0,5
0,0
-0,5
-1,0
-1500 -1000 -500 0 500 1000
-500 0 500 1000
-500 0 500 1000
H (Oe)
H (Oe)
H (Oe)

FIG. 4

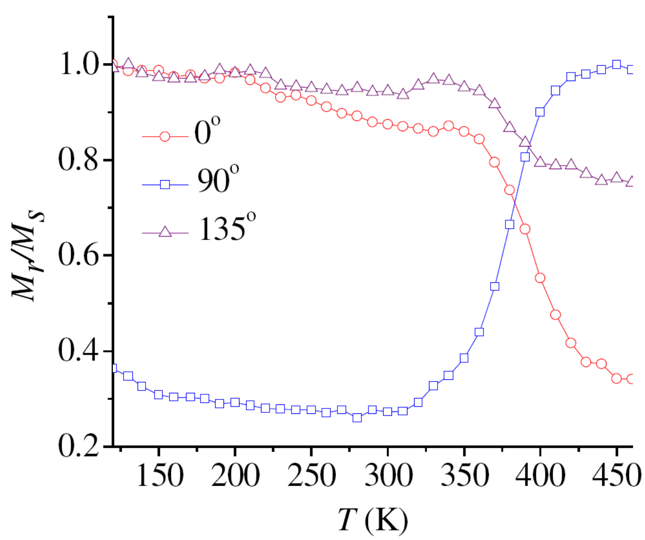

FIG. 5

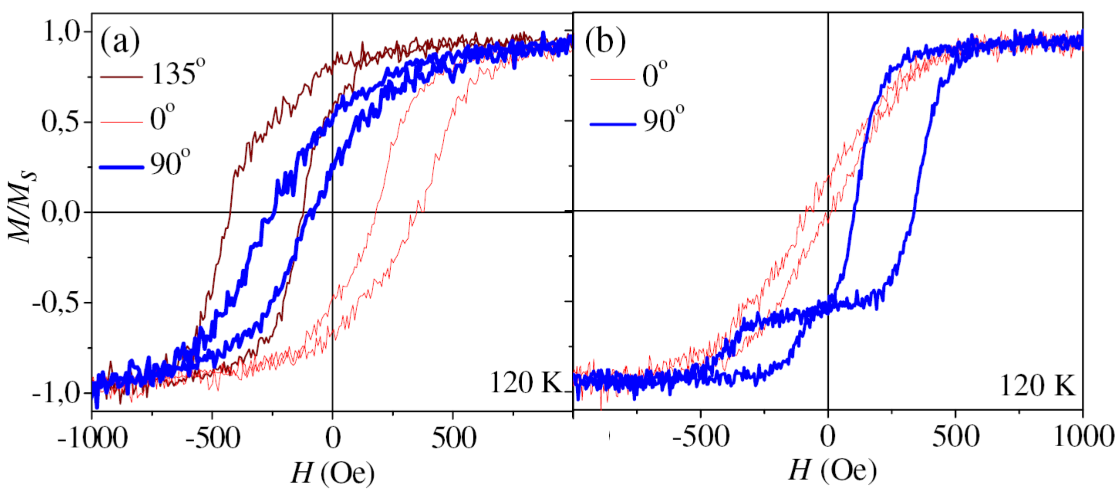

(a)
135°
0°
90°
120 K
M/M_S
1,0
0,5
0,0
-0,5
-1,0
-1000
-500
0
500
H (Oe)
(b)
0°
90°
120 K
-500
0
500
1000
H (Oe)

FIG. 6

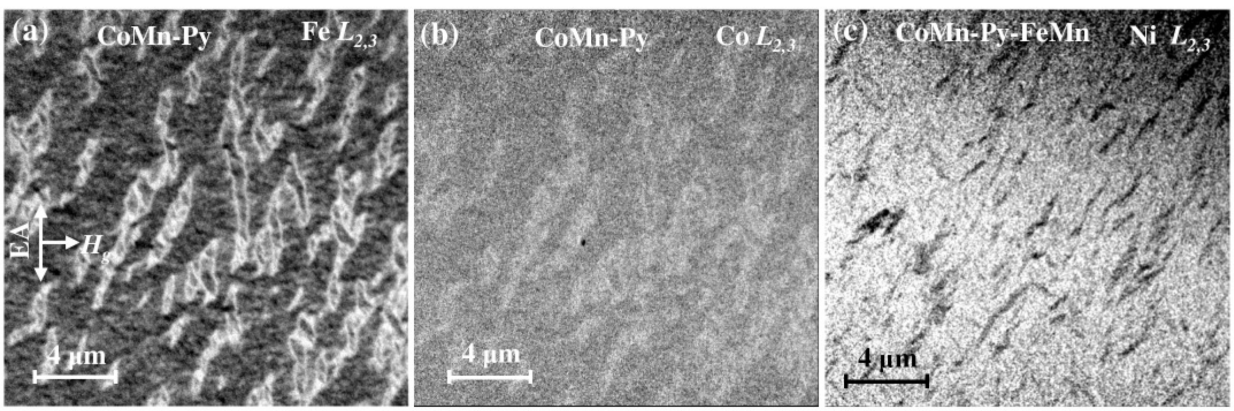

(a)
CoMn-Py
Fe $L_{2,3}$
EA
H_g
4 µm
(b)
CoMn-Py
Co $L_{2,3}$
4 µm
(c)
CoMn-Py-FeMn
Ni $L_{2,3}$
4 µm